

COMPACT DUAL-BAND 90° COUPLERS WITH CUSTOMIZABLE POWER DIVISION RATIOS UTILIZING SCRLH TRANSMISSION LINES

Jianqiang Gong^{*}, Changhong Liang, and Bian Wu

National Key Laboratory of Antennas and Microwave Technology, Xidian University, Xi'an, Shanxi 710071, China

Abstract—Novel dual-band 90° couplers with arbitrary power division ratios using simplified composite right-/left-handed (SCRLH) transmission lines (TLs) are proposed. With a degree of freedom in the structural parameters, a SCRLH stub can easily be tailored to imitate a conventional 90° section at two arbitrary frequencies with different characteristic impedances, making the resulting couplers with customizable power division ratios, as well as ensuring the size miniaturization and element realizability. To validate our idea, 90° couplers operated at 2.45/5.2 GHz with various power division ratios are designed and fabricated using microstrip technology. Good agreement is achieved between the simulated and measured results, justifying that the SCRLH configuration provides a new way of implementing compact dual-band 90° couplers with arbitrary power split ratios.

1. INTRODUCTION

Modern wireless and mobile communication systems take on a trend of multiband and miniaturization, which demands integrating multiband functionalities in a single RF component to retain compactness and possibly lower insertion loss. As is known, quadrature couplers offer 90° phase difference and equal/unequal power splitting between the output and coupling ports, having found pervasive applications in microwave and millimeter-wave circuits, such as the power combiners/dividers, balanced mixers and push-pull amplifiers, etc. Until now, a variety of techniques have been proposed to make up multiband couplers, including stub loading [1, 2], coupled lines [3, 4], stepped-impedance

Received 7 November 2012, Accepted 28 December 2012, Scheduled 3 January 2013

* Corresponding author: Jianqiang Gong (jqgongxd@gmail.com).

resonators [5, 6], port extension [7–9], metamaterials [10–12] and the fusion of the techniques referenced. However, most work have been dedicated to multiband couplers with equal power division. In practice, different coupling coefficients are often needed for different system requirements. For example, a small amount of signal needs to be coupled to a monitoring circuit at an antenna feeding port. Under such scenarios, couplers with unequal power distribution may be preferred [13–15]. In [16], a miniaturized ring $0^\circ/180^\circ$ coupler with 6 dB power division ratio was proposed by adopting the composite right-/left-handed (CRLH) transmission lines (TLs), for the high impedance imperative to the high power split ratio could be achieved with the unbalanced CRLH TL in its left-handed band. Nevertheless, due to the inherent low impedance characteristics in the right-handed band, such CRLH TL based coupler is only a single-band component.

Inspired by the idea of [16], we further extend the work of [12] to develop novel compact dual-band 90° couplers with customizable power division ratios. In [12], a 3 dB dual-band microstrip 90° coupler with good gain balance has been realized with the Simplified CRLH (SCRLH) TLs. Whereas in this paper, it will be demonstrated that by letting the characteristic impedance of the uniform TLs in the SCRLH configuration be an additional variable parameter, the modified SCRLH TL based stubs can produce vital high/low impedances at the arbitrarily specified dual frequencies, which guarantees the realizability of the targeted dual-band 90° couplers with unequal power divisions.

2. SCRLH STUB WITH DUAL-BAND PROPERTIES

The lumped circuit model of a single SCRLH TL unit cell is shown in Fig. 1(a), in which L_R is the series inductor, L_L the shunt inductor, C_R the shunt capacitor, β_s the propagation constant and p the physical length of a single unit cell. It possesses nonlinear dispersion properties and a continuous and uniform impedance distribution during the passband as illustrated in Fig. 1(b), and the passband is delimited by the lower cutoff frequency ω_{cL} and the higher cutoff frequency ω_{cH} , which can be determined by the circuit parameters L_R , L_L and C_R as [17]

$$\omega_{cL} = \frac{1}{\sqrt{L_L C_R}} \frac{1}{\sqrt{1 + \frac{L_R}{4L_L}}} \quad (1)$$

$$\omega_{cH} = \frac{1}{\sqrt{L_L C_R}} \frac{1}{\sqrt{1 + \frac{L_R}{4L_L}}} \sqrt{1 + 4 \frac{L_L}{L_R}} \quad (2)$$

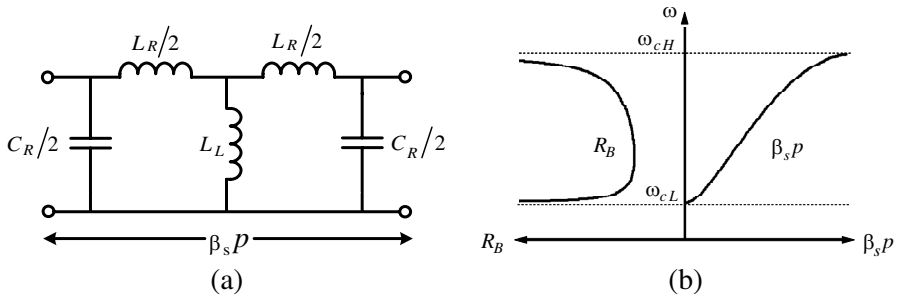


Figure 1. (a) Lumped circuit model of SCRLH TL. (b) Illustration of phase shift $\beta_s p$ per unit cell (to the right of the ω -axis) and Bloch impedance Z_B (to the left of the ω -axis) of SCRLH TL where R_B is real part of Z_B .

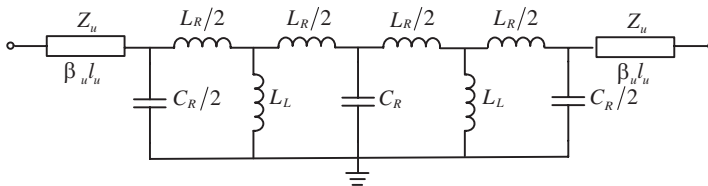


Figure 2. Generalized circuit model for dual-band stub using SCRLH TL.

It is clearly seen that the purely real Bloch impedance experiences abrupt increase near both band edges, while a relatively low and smooth impedance distribution resides at the center of the passband, which means the SCRLH TL has a wide range of impedance variation throughout the passband, essential for generating high/low impedances at arbitrary dual frequencies. However, relatively high impedance is only observed near the upper bound of the left-handed passband for the conventional unbalanced CRLH TL, which may be more suitable for single-band operation. It is this unique impedance distribution of the SCRLH TL that mainly constitutes the foundation for the dual-band 90° coupler with unequal power divisions.

The generalized circuit model of a SCRLH TL based dual-band stub is shown in Fig. 2, comprising two SCRLH TL unit cells and two uniform TL sections at lateral sides. Each uniform TL is featured by its characteristic impedance Z_u and the electrical length $\beta_u l_u$, product of the propagation constant β_u and the physical length l_u , which facilitates the interconnection of the coupler stubs and simultaneously plays roles of an impedance transformer and a phase

compensator, as will be demonstrated later. Any practical TL types can be adopted to implement the generalized circuit model, such as the microstrip line [12, 17]. Once the TL type is selected, there will be five independent variables (Z_u , $\beta_u l_u$, L_R , L_L and C_R) to be determined in order to fulfill the dual-band operation conditions. In [12], Z_u was fixed to be constant at the dual bands, while in this paper, Z_u is set to be a variable parameter, thus not only ensuring the dual-band functionalities of novel hybrid couplers with arbitrary power divisions, but also satisfying the requirements of the size reduction and element realizability.

A traditional single-band 90° coupler with arbitrary power splitting is depicted in Fig. 3, where Z_m and Z_b are the main-line and branch-line characteristic impedances respectively. If perfect matching ($S_{ii} = 0$, $i = 1, 2, 3, 4$) and isolation ($S_{41} = 0$) are required with a specified power splitting ratio $|S_{21}| - |S_{31}| = \Delta$ dB, the formulas below should be satisfied [18]

$$\frac{Z_m}{Z_0} = \frac{d}{\sqrt{1+d^2}} \quad (3)$$

$$\frac{Z_b}{Z_0} = d \quad (4)$$

where $d = 10^{\Delta/20}$ and Z_0 is the system impedance. Letting Δ_1 (dB) and Δ_2 (dB) be the respective power division ratios at f_1 and f_2 , if a dual-band branch line is implemented using the SCRLH stub, the equations below should be tenable at one time

$$\left. \begin{aligned} \phi_{bT}(f_1) &= 2(\phi_{bs}(f_1) + \phi_{bu}(f_1)) = 90^\circ \\ \phi_{bT}(f_2) &= 2(\phi_{bs}(f_2) + \phi_{bu}(f_2)) = 270^\circ \\ Z_b(f_1) &= Z_B(f_1) = Z_{b1} \\ Z_b(f_2) &= Z_B(f_2) = Z_{b2} \end{aligned} \right\} \quad (5)$$

with

$$\left. \begin{aligned} \phi_{bs} &= \beta_s p \\ \phi_{bu} &= \beta_u l_u \end{aligned} \right\}$$

where Z_{b1} and Z_{b2} can be calculated by (4) with given Δ_1 and Δ_2 . ϕ_{bT} is the total phase shift of the SCRLH branch-line stub, and ϕ_{bs} and ϕ_{bu} are the phase shifts induced by a single SCRLH TL unit cell and a single section of the uniform TL respectively. Z_B is the Bloch impedance of the SCRLH branch-line stub. The first two equations in (5) designate the requirements of phase shifts for the dual-band branch line, while the latter two describe the impedance specifications. The total transfer matrix M_T corresponding to the SCRLH branch-line

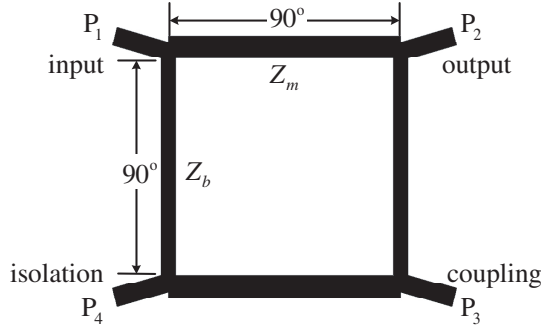


Figure 3. Schematic of classical quadrature coupler.

stub can be expressed as

$$M_T = \begin{bmatrix} a_{11} & a_{12} \\ a_{21} & a_{22} \end{bmatrix} = M_u \cdot M_s \cdot M_s \cdot M_u \quad (6)$$

with

$$M_s = \begin{bmatrix} a'_{11} & a'_{12} \\ a'_{21} & a'_{22} \end{bmatrix} \\ = \frac{1}{16L_L} \begin{bmatrix} 8L_R + 16L_L - 8\omega^2 L_R L_L C_R - 2\omega^2 L_R^2 C_R & \\ j\omega (16L_L C_R + 8L_R C_R - \frac{16}{\omega^2} - 4\omega^2 L_R L_L C_R^2 - \omega^2 L_R^2 C_R^2) & \\ j\omega (4L_R^2 + 16L_R L_L) & \\ 8L_R + 16L_L - 8\omega^2 L_R L_L C_R - 2\omega^2 L_R^2 C_R & \end{bmatrix}$$

and

$$M_u = \begin{bmatrix} \cos(\beta_u l_u) & jZ_u \sin(\beta_u l_u) \\ \frac{j}{Z_u} \sin(\beta_u l_u) & \cos(\beta_u l_u) \end{bmatrix}$$

where M_s and M_u are the transfer matrixes of the SCRLH TL unit cell and the uniform TL section, respectively. For symmetrical structures such as the SCRLH stubs, their Bloch parameters are identical to their image parameters, therefore, according to either the Floquet-Bloch theorem or the image parameter method, Z_B and ϕ_{bs} can be formulated as [19]

$$\left. \begin{aligned} Z_B &= a_{12} / \sqrt{a_{11}^2 - 1} \\ \phi_{bs} &= \cos^{-1}(a'_{11}) \end{aligned} \right\} \quad (7)$$

where a_{11} and a_{12} are the first and second elements of M_T , while a'_{11} is the first element of M_s . Based on (5) to (7), hybrid optimization

algorithm (combination of the Random and Quasi-Newton search methods) is used to solve the stub parameters. Since there are five unknowns in total, a degree of freedom exists, being helpful to achieve the circuit miniaturization as well as the element realizability. Identical synthesis procedure is also applicable to the solution of the SCRLH main-line stub parameters.

As an example, we are now to design a dual-band branch-line stub working at $f_1 = 2.45$ GHz and $f_2 = 5.2$ GHz with $Z_0 = 50 \Omega$. Microstrip is chosen to be the host substrate with relative permittivity of 2.65, loss tangent of 0.002 and thickness of 1.0 mm. Setting $\Delta_1 = 3$ dB and $\Delta_2 = 6$ dB, we can obtain $Z(f_1) = Z_{b1} = 70.6 \Omega$ and $Z(f_2) = Z_{b2} = 99.8 \Omega$ from (4). Then establishing a fitness function with (5) to (7) in the hybrid optimization algorithm, after optimization, moderate circuit element values of the branch-line stub can be obtained, as listed in Table 1 for stub Z_b of coupler A. With these theoretical values, the practical microstrip SCRLH stub can further be engineered using the topology synthesis method presented in [17]. Fig. 4(a) shows the microstrip layout with optimized dimensions of $w_u = 1.2$ mm, $l_u = 5.5$ mm, $w_1 = 8.0$ mm, $w_2 = 0.9$ mm, $w_3 = 0.35$ mm, $l_1 = 5.0$ mm, $l_2 = 0.9$ mm, $l_3 = 1.25$ mm and $l_4 = 2.63$ mm. Comparing the HFSS calculated Z_B and ϕ_{bT} with their corresponding theoretical values calculated from (5) to (7) using the ideal circuit element values, good agreement among these results is clearly seen in Fig. 4(b), verifying that the generalized circuit model in Fig. 2 can be effectively implemented using the microstrip

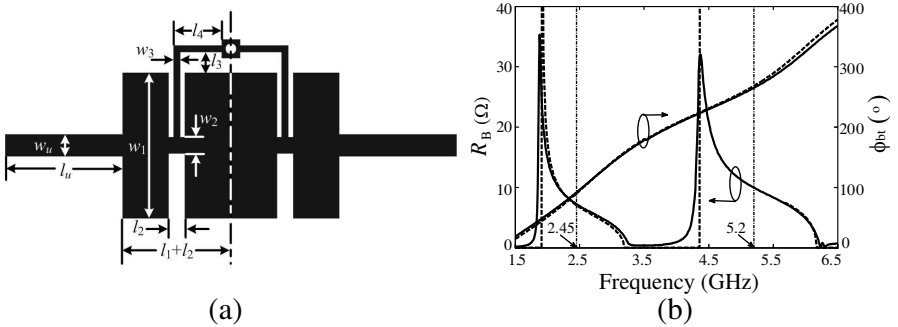


Figure 4. (a) Dual-band microstrip SCRLH stub. (b) HFSS-Calculated SCRLH stub Bloch impedance Z_B and phase shift ϕ_{bT} (solid line), and R_B is the real part of Z_B . The corresponding theoretical results from (5) and (6) are represented with the dashed line, respectively.

configuration in Fig. 4(a). Moreover, it can be read from the full-wave curves that the designed microstrip stub presents calculated Bloch impedances of 72.4Ω and 100.8Ω with total phase shifts of 91.8° and 267.5° at 2.45 GHz and 5.2 GHz, respectively, attaining almost perfectly consistent specifications as required in (5).

3. DUAL-BAND 90° COUPLERS WITH ARBITRARY POWER DIVISION RATIOS

With the proposed synthesis method for the SCRLH stubs, two microstrip 90° couplers with different power divisions are designed at the WLAN dual frequencies. The first quadrature coupler (Coupler A) is designed to have $\Delta_1 = 3$ dB and $\Delta_2 = 6$ dB, while the second one (Coupled B) has $\Delta_1 = 6$ dB and $\Delta_2 = 3$ dB. Coupler circuit parameters obtained through the hybrid optimization are listed in Table 1, while the corresponding physical parameters are exhibited in Table 2. All full-wave simulations are carried out by Ansoft HFSS. It is observed that Z_m stubs for both couplers have close circuit and physical parameters, while Z_b stub parameters have more distinct values, since each Z_b stub has to implement relatively high characteristic impedances with distinct values at the dual frequencies. Due to the discontinuities introduced by the stub interconnections, the

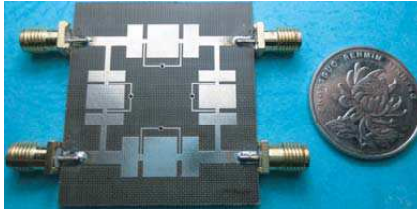
Table 1. Circuit parameters of the two designed dual-band 90° couplers with different power divisions.

Coupler	Δ_1	Δ_2	Stub	Z_u (Ω)	$\beta_u l_u$ ($^\circ$)	L_R (nH)	L_L (pF)	C_R (pF)
A	3	6	Z_m	45.0	14.6	1.2	3.4	2.0
			Z_b	85.0	25.0	1.2	3.5	1.4
B	6	3	Z_m	40.0	18.3	1.2	3.4	1.8
			Z_b	72.8	25.5	2.2	6.2	0.8

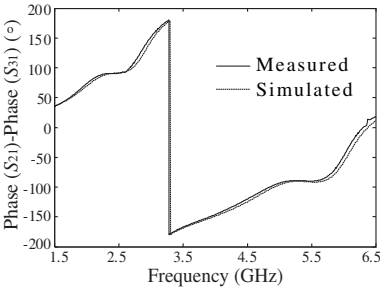
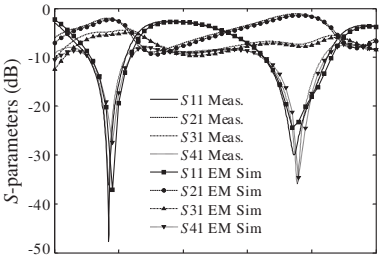
Table 2. Physical parameters of the two microstrip dual-band 90° couplers with different power divisions.

Coupler	Stub	w_u	l_u	w_1	w_2	w_3	l_1	l_2	l_3	l_4
A	Z_m	2.58	3.9	8.0	1.40	0.35	7.0	0.9	1.55	3.63
	Z_b	1.20	5.4	8.0	0.90	0.35	5.0	0.9	1.15	2.63
B	Z_m	2.58	3.6	8.0	0.80	0.35	6.8	1.0	1.65	3.58
	Z_b	1.30	5.6	8.0	0.25	0.45	4.0	1.3	0.90	2.38

physical parameters of the Z_b stub of Coupler A in Table 2 are of minor difference from those presented in the previous segment. According to the listed physical parameters, both couplers are experimentally fabricated and tested. Fig. 5 and Fig. 6 show their respective prototype photographs and frequency responses. Fig. 5(b) and Fig. 6(b) compare the measured results of $|S_{11}|$, $|S_{21}|$, $|S_{31}|$, $|S_{41}|$ and $\angle S_{21} - \angle S_{31}$ with the simulation data and detailed response values are listed in Table 3. For Coupler A, the measurement shows that $\Delta_1 = 2.2$ dB

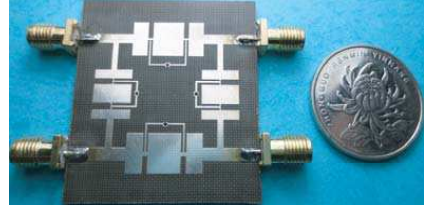


(a)

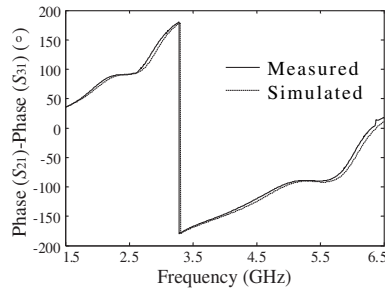
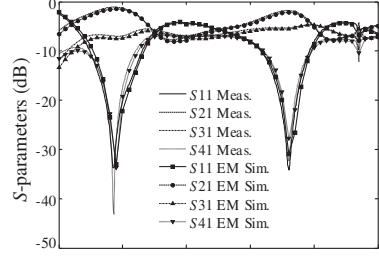


(b)

Figure 5. Performances of Coupler A with $\Delta_1 = 3$ dB and $\Delta_2 = 6$ dB at 2.45 GHz and 5.2 GHz, respectively. (a) Photograph of the fabricated prototype. (b) Magnitude of S_{11} , S_{21} , S_{31} , S_{41} and phase difference between S_{21} and S_{31} .



(a)



(b)

Figure 6. Performances of Coupler B with $\Delta_1 = 6$ dB and $\Delta_2 = 3$ dB at 2.45 GHz and 5.2 GHz, respectively. (a) Photograph of the fabricated prototype. (b) Magnitude of S_{11} , S_{21} , S_{31} , S_{41} and phase difference between S_{21} and S_{31} .

and $\Delta_2 = 6.0$ dB, and the error of Δ_1 (0.8 dB) might be caused by the fabrication tolerance, and additionally, the phase of output signal leads at f_1 and lags at f_2 compared to that of coupling signal. The measured relative phase deviations $\angle S_{21} - \angle S_{31} - 90^\circ$ at f_1 and $\angle S_{21} - \angle S_{31} + 90^\circ$ at f_2 are only 0.4° and 0.7° , respectively. Likely for Coupler B, the measured data demonstrate $\Delta_1 = 5.8$ dB and $\Delta_2 = 3.2$ dB, and $\angle S_{21} - \angle S_{31} - 90^\circ$ at f_1 and $\angle S_{21} - \angle S_{31} + 90^\circ$ at f_2 are merely -0.6° and 2.1° , respectively. Their respective circuit bandwidths are listed in Table 4. The bandwidths are defined by the frequencies where $|S_{11}| < -15$ dB, $|S_{41}| < -15$ dB, $|S_{21}|/|S_{31}| - \Delta_i = \pm 0.5$ dB, and $\angle S_{21} - \angle S_{31} \mp 90^\circ = \pm 5^\circ$. For Coupler A, the bandwidths at f_1 and f_2 are mainly of the same order, but for Coupler B, the relative bandwidths at f_1 are often much larger than those at f_2 . Coupler A has a dimension of $0.21\lambda \times 0.22\lambda$ and Coupler B is $0.20\lambda \times 0.21\lambda$ in size, where λ is guided wavelength of the 50Ω microstrip line at f_1 . If all C_R elements in Fig. 2 is implemented using lumped components instead of the low-impedance line, couplers with more compact size can be achieved, but larger insertion losses may be resulted at the same time. In short, the measured results agree well with the simulated ones, and both SCRLH coupler prototypes display good electrical properties.

Further comparing the fabricated devices with the two couplers constructed using the SIR stub loading techniques in [13], our devices exhibit comparable return losses and isolations, but slightly higher insertion losses, mainly stemming from the radiation losses caused by

Table 3. Circuit performances of the two microstrip dual-band hybrid couplers with different power divisions.

	Coupler A	
	Sim.	Meas.
S_{11} (dB)	-25.0/ - 24.4	-19.0/ - 29.1
S_{21} (dB)	-2.3/ - 1.5	-2.4/ - 1.2
S_{31} (dB)	-5.3/ - 7.6	-4.6/ - 7.2
S_{41} (dB)	-21.8/ - 21.2	-17.1/ - 24.8
$\angle S_{21} - \angle S_{31}$ ($^\circ$)	91.0/ - 90.9	90.4/ - 89.3
	Coupler B	
	Sim.	Meas.
S_{11} (dB)	-25.9/ - 26.6	-23.2/ - 22.2
S_{21} (dB)	-1.5/ - 2.3	-1.2/ - 2.0
S_{31} (dB)	-7.5/ - 5.3	-7.0/ - 5.2
S_{41} (dB)	-24.0/ - 22.0	-21.2/ - 20.1
$\angle S_{21} - \angle S_{31}$ ($^\circ$)	90.2/ - 89.3	89.4/ - 87.9

Table 4. Bandwidth (%) of the two microstrip dual-band hybrid couplers with different power divisions.

Coupler		$ S_{21} / S_{31} $ ($\Delta_i \pm 0.5$ dB)	$\angle S_{21} - \angle S_{31}$ $\mp 90 \pm 5^\circ$	$1/ S_{11} $ (> 15 dB)	$1/ S_{41} $ (> 15 dB)
A	Sim.	28.1/9.1	17.7/14.4	14.1/12.5	12.5/9.5
	Meas.	9.0/8.4	19.4/14.2	13.5/12.1	12.1/9.6
B	Sim.	14.1/8.9	26.7/9.2	20.4/8.5	16.7/7.0
	Meas.	11.4/9.7	26.8/9.3	21.5/8.6	15.6/7.1

the grounded vias. Bandwidth of Coupler A is comparable in the first band, but smaller in the second band, whereas for Coupler B, bandwidth is smaller in the first band, but larger in the second band. It is worth restating that our method has a foothold in the application of the dispersion and Bloch impedance characteristics of the metamaterial structures, while the SIR stub loading techniques in [13] still bases on the traditional microwave network equivalence, therefore, our work may be a stimulus for engineers to design more useful microwave components from the metamaterial viewpoints.

4. CONCLUSIONS

In this paper, the dual-band 90° couplers with arbitrary power splitting ratios have been designed based on the SCRLH TLs. The SCRLH TL features nonlinear dispersion properties and relatively wide range of impedance variation during its passband, and a degree of freedom exists in the SCRLH stub configuration, ensuring the successful synthesis of the dual-band stub with the specified phase shifts and characteristic impedances. The hybrid optimization algorithm has been adopted to solve the parameters of the SCRLH stub. Due to a degree of freedom, the obtained parameters can be chosen freely to be implemented conveniently using microwave components. To verify the design methodology, two microstrip hybrid couplers with different power divisions working at the WLAN dual bands have been successfully synthesized, featuring good operational performances.

ACKNOWLEDGMENT

This work was supported by the Fundamental Research Funds for the Central Universities No. K5051202007 and by the National Natural Science Foundation of China (NSFC) under project No. 61271017.

REFERENCES

1. Cheng, K.-K. M. and F.-L. Wong, "A novel approach to the design and implementation of dual-band compact planar 90° branch-line coupler," *IEEE Trans. Microw. Theory Tech.*, Vol. 52, No. 11, 2458–2463, Nov. 2004.
2. Chin, K.-S., K.-M. Lin, Y.-H. Wei, T.-H. Tseng, and Y.-J. Yang, "Compact dual-band branch-line and rat-race couplers with stepped-impedance-stub lines," *IEEE Trans. Microw. Theory Tech.*, Vol. 58, No. 5, 1213–1221, May 2010.
3. Yeung, L. K., "A compact dual-band 90° coupler with coupled-line sections," *IEEE Trans. Microw. Theory Tech.*, Vol. 59, No. 9, 2227–2232, Sep. 2010.
4. Wan, X., W.-Y. Yin, and K.-L. Wu, "A dual-band coupled-line coupler with an arbitrary coupling coefficient," *IEEE Trans. Microw. Theory Tech.*, Vol. 60, No. 4, 945–951, Apr. 2012.
5. Kuo, J.-T. and C.-H. Tsai, "Generalized synthesis of rat race ring coupler and its application to circuit miniaturization," *Progress In Electromagnetics Research*, Vol. 108, 51–64, 2010.
6. Nosrati, M. and M. Daneshmand, "Dual-wideband branch-line coupler based on a loaded N-segment SIR," *Micro. Opt. Technol. Lett.*, Vol. 54, No. 10, Oct. 2012.
7. Kim, H., B. Lee, and M.-J. Park, "Dual-band branch-line coupler with port extensions," *IEEE Trans. Microw. Theory Tech.*, Vol. 58, No. 3, 651–655, Mar. 2010.
8. Lin, F. and Q.-X. Chu, "A novel tri-band branch-line coupler with three controllable operating frequencies," *IEEE Microw. Wireless Compon. Lett.*, Vol. 20, No. 12, 666–668, Dec. 2010.
9. Wong, Y. S., S. Y. Zheng, and W. S. Chan, "Multifolded bandwidth branch line coupler with filtering characteristics using coupled port feeding," *Progress In Electromagnetics Research*, Vol. 118, 17–35, 2011.
10. Lin, I.-H., M. DeVincentis, C. Caloz, and T. Itoh, "Arbitrary dual-band components using composite right/left-handed transmission lines," *IEEE Trans. Microw. Theory Tech.*, Vol. 52, No. 4, 1142–1149, Apr. 2004.
11. Bonache, J., G. Sisó, M. Gil, Á. Iniesta, J. García-Rincón, and F. Martín, "Application of composite right-left handed (CRLH) transmission lines based on complementary split ring resonators (CSRRS) to the design of dual-band microwave components," *IEEE Microw. Wireless Compon. Lett.*, Vol. 18, No. 8, 524–526, Aug. 2008.

12. Gong, J.-Q., C.-H. Liang, and B. Wu, "Novel dual-band hybrid coupler using improved simplified CRLH transmission line stubs," *Micro. Opt. Technol. Lett.*, Vol. 52, No. 11, Nov. 2010.
13. Hsu, C.-L., J.-T. Kuo, and C.-W. Chang, "Miniaturized dual-band hybrid couplers with arbitrary power division ratios," *IEEE Trans. Microw. Theory Tech.*, Vol. 57, No. 1, 149–156, Jan. 2009.
14. Lin, F., Q.-X. Chu, and S. W. Wong, "Compact broadband microstrip rat-race couplers using microstrip/slotline phase inverters for arbitrary power dividing ratios," *Journal of Electromagnetic Waves and Applications*, Vol. 26, Nos. 17–18, 2012.
15. Li, B. and W. Wu, "Compact dual-band branch-line coupler with 20 : 1 power dividing ratio," *Journal of Electromagnetic Waves and Applications*, Vol. 25, No. 4, 607–615, Apr. 2011.
16. Chi, P.-L., "Miniaturized ring coupler with arbitrary power divisions based on the composite right/left-handed transmission lines," *IEEE Microw. Wireless Compon. Lett.*, Vol. 22, No. 4, 170–172, Apr. 2012.
17. Gong, J.-Q. and Q.-X. Chu, "SCRLH TL based UWB bandpass filter with widened upper stopband," *Journal of Electromagnetic Waves and Applications*, Vol. 22, Nos. 14–15, 1985–1992, 2008.
18. Matthaei, G. L., L. Young, and E. M. T. Jones, *Microwave Filters, Impedance-Matching Network, and Coupling Structures*, Artech House, Norwood, MA, 1980.
19. Pozar, D. M., *Microwave Engineering*, 3rd Edition, Publishing House of Electronics Industry, Beijing, 2006.